GCM Estimate of the Indirect Aerosol Forcing Using Satellite-Retrieved Cloud Droplet Effective Radii

OLIVIER BOUCHER

Laboratoire de Météorologie Dynamique du CNRS, Ecole Normale Supérieure, Paris, France

(Manuscript received 12 July 1994, in final form 8 November 1994)

ABSTRACT

In a recent paper, Han et al. analyzed satellite data radiances to retrieve cloud droplet effective radii and reported significant interhemispheric differences for both maritime and continental clouds. The mean cloud droplet radius in the Northern Hemisphere is smaller than in the Southern Hemisphere by about 0.7 μm. This hemispheric contrast suggests the presence of an aerosol effect on cloud droplet size and is consistent with higher cloud condensation nuclei number concentration in the Northern Hemisphere due to anthropogenic production of aerosol precursors. In the present study, we constrain a climate model with the satellite retrievals of Han et al. and discuss the climate forcing that can be inferred from the observed distribution of cloud droplet radius. Based on two sets of experiments, this sensitivity study suggests that the indirect radiative forcing by anthropogenic aerosols could be about -0.6 or -1 W m^{-2} averaged in the 0°–50°N latitude band. The uncertainty of these estimates is difficult to assess but is at least 50%.

1. Introduction

In addition to their direct effect (i.e., backscattering of sunlight in clear sky), it is believed that anthropogenic aerosols stemming from industrial SO_2 emissions could alter the distribution and concentration of cloud condensation nuclei (CCN) on which cloud droplets nucleate. If the same amount of liquid water is distributed among a larger number of droplets, each of the droplets will be smaller in size and cloud albedo will be increased (Twomey 1974, 1977). This effect is referred to as the indirect or "Twomey" effect. Several observational studies support, in different extents, the capability of anthropogenic aerosols to modify cloud optical properties. "Ship track" observations suggest that, under certain conditions, ship-produced aerosols increase cloud reflectivity (Coakley et al. 1987) while decreasing cloud droplet size and increasing liquid water content (Radke et al. 1989; King et al. 1993). Measurements of CCN concentrations in the marine boundary layer showed some correlation between sulfate aerosol mass and the number of CCN at a given supersaturation (Hegg et al. 1993; Berresheim et al. 1993; Quinn et al. 1993, and others). Leaitch et al. (1992b) found positive correlations between cloud water sulfate concentration and cloud droplet number concentration for continental stratiform and cumuliform clouds. Examination of Earth Radiation Budget Experiment (ERBE) satellite data (Falkowski et al. 1992; Kim and Cess 1993), however, indicates that the increase in cloud albedo over the ocean might be limited to oceanic regions adjacent to industrialized continents. Some general circulation model (GCM) modeling studies, where cloud droplet number concentration is empirically related to model-predicted sulfate mass concentration, showed that the indirect forcing caused by anthropogenic sulfate aerosols could be substantial (Boucher and Lohmann 1995; Jones et al. 1994). However, these studies suffer from the very tentative relationship that exists between sulfate aerosol mass and cloud droplet number concentration (Penner et al. 1994).

Recently, Han et al. (1994; hereafter referred to as HRL) reported that cloud droplet effective radii of the Northern Hemisphere (NH) were smaller than that of the Southern Hemisphere (SH). The hemispheric difference is higher over land (0.8 μm) than over ocean (0.4 μm). Since most anthropogenic sources of aerosols and aerosol precursors are situated in the NH, the observed hemispheric contrast in cloud droplet size might be an evidence of the effect of anthropogenic aerosols on clouds. In this study, we estimate the climate forcing implied by the observed hemispheric contrast in cloud droplet radii and discuss the implications of the HRL study in view of our simulations. We also discuss the uncertainties of our method and make rough estimates of them when possible.

2. Method

HRL performed satellite retrievals of cloud droplet effective radii using the International Satellite Cloud

Corresponding author address: Mr. Olivier Boucher, Laboratoire de Météorologie Dynamique du CNRS, Ecole Normale Supérieure de Paris, 24 rue Lhomond, Paris 75231, Cedex 05, France.
E-mail: boucher@lmd.ens.fr

Climatology Project (ISCCP) CX dataset. The dataset consists of radiances from all five channels of *NOAA-9* and *NOAA-10* AVHRRs (Advanced Very High Resolution Radiometer), as well as retrieved cloud optical depth, cloud-top temperature, cloud-top pressure, surface temperature, and reflectivity. The HRL study is restricted to clouds for which top temperature is above 0°C in order to eliminate ice clouds from the computations. Cloud droplet effective radius was first set to 10 μm, the assumed value in all ISCCP retrieval algorithms, and approximated successively to a final value with an iterative algorithm using radiances from AVHRR channels 3 and 4, in addition to ISCCP-retrieved data based on channel 1 and 4 radiances. Their results showed that droplet radii of maritime clouds were larger than those of continental clouds. They also observed that droplet radii were larger in the SH than in the NH for both continental and maritime clouds. The zonally averaged cloud droplet effective radii are shown in Fig. 1 for the year 1987 and for the *NOAA-9* satellite ("afternoon" orbiter).

We have constrained here the LMD (Laboratoire de Météorologie Dynamique) GCM with the zonally averaged cloud droplet effective radii reported by HRL. We assume that the hemispheric contrast in effective radius is due to the presence of anthropogenic aerosols (see section 5 for a discussion of this assumption). We compute the shortwave component of the cloud radiative forcing (CRF) at each latitude and longitude of the NH, with cloud droplet effective radius prescribed once to its NH latitudinal value and once to its SH latitudinal value. For this purpose, we use the zonally averaged—land or ocean—value of the cloud droplet radius at the given latitude of the NH and at the counterpart latitude of the SH. The difference in CRF, denoted ΔF, isolates our estimate of the indirect radiative forcing. Formally, ΔF at longitude θ and latitude φ ($0° < \varphi < 50°$) can be written as

$$\Delta F(\theta, \varphi) = \mathrm{CRF}[X_i(\theta, \varphi), r_e(\varphi)] - \mathrm{CRF}[X_i(\theta, \varphi), r_e(-\varphi)], \quad (1)$$

where $X_i(\theta, \varphi)$ is the vector of quantities needed to compute the CRF at point (θ, φ), except the cloud droplet effective radius, and $r_e(\varphi)$ is the zonally averaged cloud droplet radius at latitude φ, which is taken to its land/ocean value depending whether (θ, φ) defines a land or an ocean point.

Five experiments have been performed: an "annual" run and four "seasonal" runs (referred to as winter, spring, summer, and autumn[1]). The model is run 12 months in the annual experiment and one month (January, April, July, and October) in each of the seasonal experiments. We use NH and SH annually[2] and zonally averaged cloud droplet effective radii (Fig. 1a) in the annual run, NH January and SH July cloud droplet radii (Fig. 1b) in the winter experiment, NH April and SH October cloud droplet radii (Fig. 1c) in the spring experiment, and so on for the summer and the autumn experiments (Figs. 1d,e).

3. Short model description

The LMD GCM has been described in Sadourny and Laval (1984) and Le Treut and Li (1991). Cloud water is a prognostic variable of the model. Fractional cloudiness is allowed to form in the horizontal but clouds are assumed to fill the whole layer in the vertical. The main features of the radiation code are discussed below. It is based on a two-stream method of the radiative transfer equations with two spectral intervals in the solar spectrum (0.25–0.68 μm) and six in the terrestrial infrared spectrum (0.68–4.0 μm) (Morcrette 1989; Fouquart and Bonnel 1980). The scheme requires the knowledge of optical depth, asymmetry parameter, and single scattering albedo of clouds in each of the two solar bands. Distinction between liquid and ice water is temperature based with a linear transition between liquid and ice clouds between 0° and −40°C. Cloud optical depth is the sum of the optical depths for warm and cold clouds:

$$\tau = x\tau_w + (1 - x)\tau_c \quad (2)$$

$$\tau = x\frac{3}{2}\frac{W_{\text{model}}}{r_e} + (1 - x)\frac{3}{2}\frac{W_{\text{model}}}{r_{\text{ice}}}, \quad (3)$$

where W is the vertically integrated, model-predicted liquid water path in a cloud layer, and x is the mass fraction of water that is liquid. The warm cloud droplet effective radius r_e is prescribed to 10 μm to compute the radiative heating that drives the GCM and to the zonally averaged retrieved values for the diagnostic computations explained above. The ice-cloud droplet (crystal) effective radius r_{ice} is set to 25 μm. The asymmetry parameter (for warm clouds) g is a constant in each of the two spectral bands and has been computed using a high-resolution spectral model:

$$\left.\begin{aligned} g_1 &= 0.865 \\ g_2 &= 0.910 \end{aligned}\right\}. \quad (4)$$

The single scattering albedo (for warm clouds) ω is an empirical function of cloud optical depth to account for the saturation of the liquid water absorption bands (Fouquart and Bonnel 1980):

$$\left.\begin{aligned} \omega_1 &= 0.9999 - 5.\ 10^{-4}\exp(-0.5\tau) \\ \omega_2 &= 0.9988 - 2.5\ 10^{-3}\exp(-0.05\tau) \end{aligned}\right\}. \quad (5)$$

[1] By winter, for instance, we mean Northern Hemisphere January and Southern Hemisphere July.

[2] The annual average is actually a four-month average over January, April, July, and October 1987.

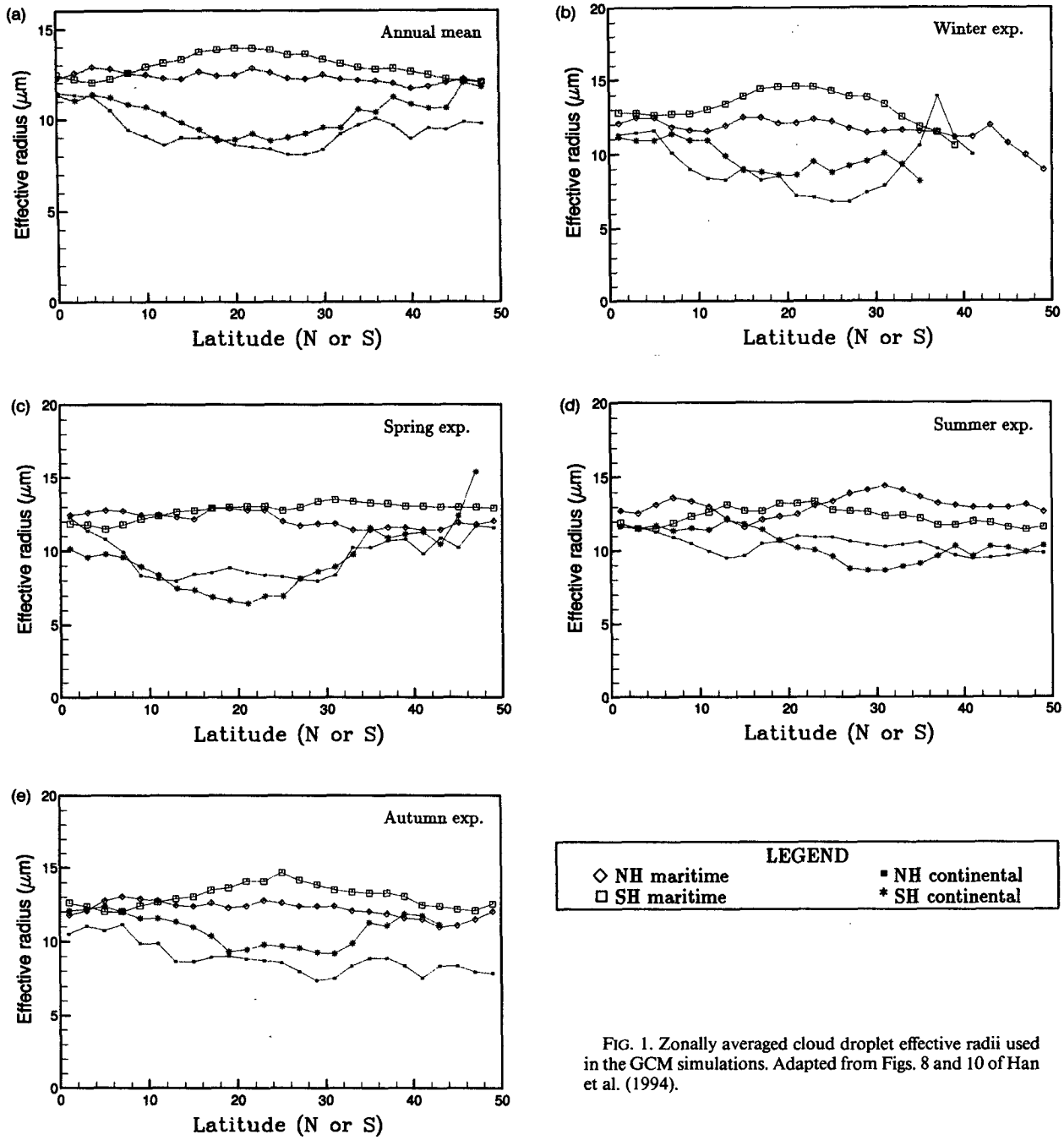

FIG. 1. Zonally averaged cloud droplet effective radii used in the GCM simulations. Adapted from Figs. 8 and 10 of Han et al. (1994).

4. Results

For the sake of concision, we show only the simulated and observed annually and zonally averaged-shortwave CRFs in Fig. 2. The latitudinal dependence of the CRF is well simulated, although the CRF is overestimated in the Tropics. The seasonal cycle (not shown here) is also well reproduced, and the simulated monthly hemispheric averages of the CRF are in fair agreement with ERBE data (Hartmann 1993).

The differences in CRFs computed with NH and SH cloud droplet effective radii (interpreted as an estimate of the aerosol indirect radiative forcing) are displayed in Table 1 and Fig. 3. The computed forcings over land are for information only because their meaning is limited due to the relative paucity of continents in the SH. For the 1-yr experiment, we simulate a negative indirect

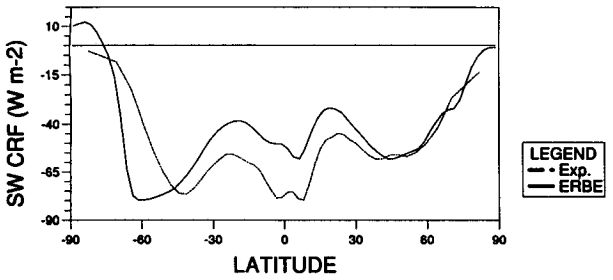

FIG. 2. Annually and zonally averaged shortwave cloud radiative forcing (W m^{-2}) from the model (dotted line) and ERBE data (solid line).

radiative forcing of -1 W m^{-2} in the 0°–50°N latitude band, with somewhat larger values over the ocean (-1.2 W m^{-2}) than over land (-0.9 W m^{-2}). The simulated forcings are larger in the winter and autumn experiments because the hemispheric contrast in cloud droplet radius is larger (up to 3 μm over ocean). In the summer experiment, we get a negative forcing over land of the same magnitude than in the winter experiment but a positive forcing over ocean, in a manner that is consistent with the prescribed distribution of cloud droplet radius. It is interesting to note that the average of the four seasonal forcings (-0.6 W m^{-2}) is smaller than the 1-yr experiment forcing (-1.0 W m^{-2}). This is because the forcing is a nonlinear function of changes in droplet size and shows how important it is to model the seasonal cycle of the various cloud-related quantities for the indirect forcing calculations. Concurrently, Leaitch et al. (1992a) and Leaitch and Isaac (1994) reported seasonal variation in the linking of sulfate aerosol mass to cloud droplet number concentration, and Tselioudis et al. (1993) showed that the temperature dependence of cloud optical depth varies with the seasons. This seasonal variability in cloud properties can potentially leave its mark on the indirect aerosol forcing. Temperature trend analysis should help to identify the seasonal variations in the forcing (Engardt and Rodhe 1993; Hunter et al. 1993), but direct and indirect radiative forcings cannot be dissociated in this context.

5. Limitations

We would like in this section to qualify the assertion that the difference in fluxes we compute [ΔF in Eq. (1)] represents an estimate of the indirect radiative forcing by anthropogenic aerosols in the NH.

1) The indirect effect might have a nonnegligible component in the SH because clouds of the SH may be more susceptible[3] (Taylor and McHaffie 1994; Jones et al. 1994; Boucher and Lohmann 1995). The computed forcings would therefore be a lower bound.

2) The hemispheric contrast in droplet radius is not necessarily due to anthropogenic aerosols only. Maritime clouds of the NH are more influenced by continental air and natural continental CCN than maritime clouds of the SH simply because there are more continents in the NH than in the SH. For this reason, the computed forcings could be as well an upper bound.

3) Other differences between clouds of the two hemispheres, such as differences in their liquid water content or vertical extent, can modify or mask the effect of enhanced cloud albedo due to changes in CCN concentration and droplet size (Han et al. 1994). This could be the reason why Schwartz (1988) did not find any interhemispheric difference, neither in the annually averaged total albedo nor in the cloud component of this albedo, which was consistent with a possible anthropogenic aerosol effect on the radiative budget. However, Schwartz's conclusion does not refute the possibility of an aerosol effect on cloud albedo.

4) The present calculations assume that liquid water content is not modified by enhanced CCN concentrations. Some microphysical feedbacks could occur because precipitation development is highly dependent on the cloud droplet spectrum. Also, this approach does not take into account the possible change in cloud colloidal stability and lifetime suggested by Albrecht (1989) and Parungo et al. (1994).

5) There are no satellite data at latitudes higher than 50°. The forcing in the high latitudes of the NH can be important because of the large CRF between 50° and 70°N in the summertime.

6) ISCCP data are representative of the cloud-top layer and give little information on the vertical structure of cloud properties. This weakness is actually less restrictive than it may appear because we only consider low-level clouds (such as stratocumulus), which are defined unambiguously in both the satellite data and the GCM.

Other cloud optical properties such as the asymmetry parameter or the single scattering albedo are prescribed to different values in the ISCCP and GCM radiative transfer models. These inconsistencies introduce systematic biases in our results but these must remain small because Mie optical properties of droplets are well known (in contrast maybe to optical properties of ice crystals).

TABLE 1. Mean simulated forcings (W m^{-2}).

	1-yr expt.	Winter	Spring	Summer	Autumn
0–50°N					
land/ocean	−1.0	−1.25	−0.65	+0.9	−1.4
ocean	−1.1	−1.75	−1.05	+1.5	−1.25
land	−0.9	−0.35	+0.1	−0.3	−1.6

[3] Cloud susceptibility is defined by Platnick and Twomey (1994) as the derivative of cloud albedo with respect to cloud droplet number concentration.

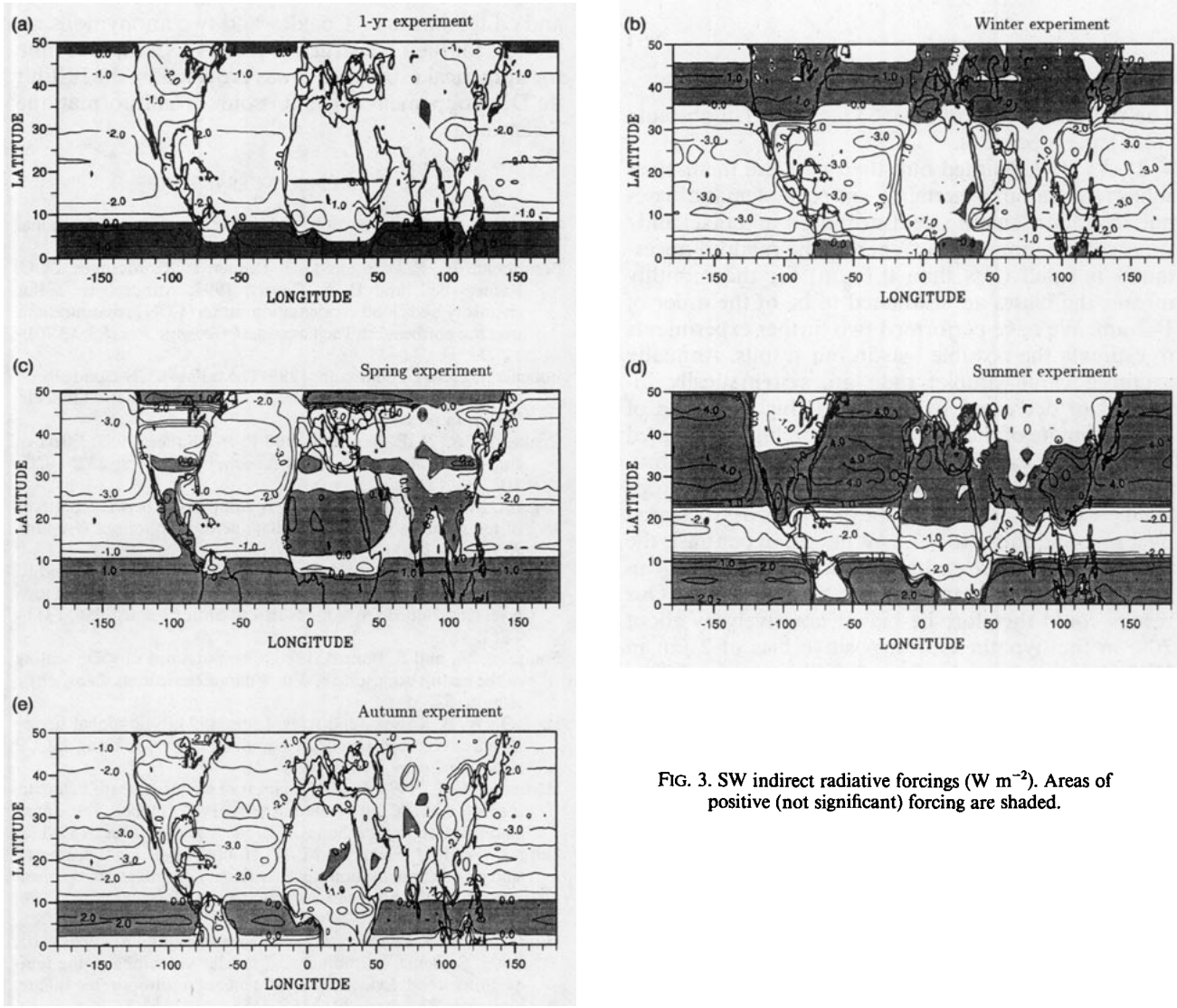

FIG. 3. SW indirect radiative forcings (W m^{-2}). Areas of positive (not significant) forcing are shaded.

7) Because CRF is a nonlinear function of cloud droplet radius and because of the natural variability in cloud droplet effective radius, we are biasing our results by considering a mean value for the cloud droplet effective radius instead of a probability distribution. We use our radiation model in its off-line version to perform single-column computations of radiative fluxes and test the effect of considering a probability distribution of droplet effective radii instead of 2° × 2° monthly means. For this purpose we use the distributions of the frequency of cloud droplet effective radius values in the 40°–50°N latitude zone for January and July as derived by HRL (their Fig. 6). These probability distributions reflect the variability in space for scales larger than the spacing between sampled AVHRR pixels (i.e., about 30 km × 30 km) and the variability in time for timescales larger than the sampling period (i.e., one day). Although it would have been more appropriate to catch more of the variability in time (i.e., to have a shorter sampling period), the use of these probability distributions gives an indication of how sensitive our results are to the averaging procedure. We compute the CRF using this probability distribution, the same probability distribution shifted toward 1 μm smaller radii and the corresponding mean radii. The computations are performed for a variety of situations using GCM-simulated vertical profiles of temperature, cloudiness, and liquid water content. The difference in forcings is about 20% to 40% higher for the full calculations (i.e., using the probability distributions) than for the calculations using the mean effective radii. This is because the change in forcing for a given change in droplet radius is larger at small droplet effective radii than at large ones, as shown by the expression of the derivative of τ with respect to r_e in our simple parameterization:

$$\frac{\partial \tau}{\partial r_e} = -\frac{x\tau_w}{r_e}. \quad (6)$$

The right-hand side of Eq. (6) increases (in absolute value) as r_e decreases.

8) As HRL pointed out, their data are themselves subject to random uncertainty and/or systematic biases due to cloud-element size distribution in a pixel and/or cirrus contamination. Whereas the random uncertainty is small (less than 0.1 μm) for the monthly means, the biases are estimated to be of the order of 1–2 μm. We have performed two further experiments to estimate the possible bias in our results. Annually averaged cloud droplet radii are systematically increased or decreased by 2 μm (the higher bound of HRL estimate of the bias) and the forcing is estimated as in the 1-yr experiment described above. The simulated forcing (averaged between 0° and 50°N) drops from -1.0 to -0.9 W m^{-2} if the droplet size is increased by 2 μm, and raises to -1.2 W m^{-2} if, in contrast, the droplet size is decreased by the same value. This can be explained by the same considerations as above. Our results could therefore be biased negatively by about 20% in the hypothesis of a positive bias of 2 μm in HRL data but even the sign of this bias is not clear.

6. Conclusions

The use of satellite-retrieved cloud droplet radii in a climate model shows that the aerosol indirect radiative forcing could be substantial (between -0.6 and -1 W m^{-2} in the 0°–50°N latitude band) if we attribute the observed hemispheric contrast in cloud droplet radius to the effect of anthropogenic aerosols on cloud properties. The multiplicity and diversity of the assumptions made here make it difficult to quantify the uncertainty on this estimate. Only two sources of errors have been quantified, giving uncertainties of 20%–40% and 10%–20%, respectively. However, it is remarkable that this estimate is in the range given by Boucher and Lohmann (1995) and close to that of Jones et al. (1994), although the geographical and temporal distributions of the forcing are different. We further conclude that the HRL data translate into a strong seasonal cycle in terms of radiative forcing. Insolation has a direct effect on the magnitude of the forcing but also an indirect effect through the dependence of cloud properties on temperature and convective activity. Therefore, the forcing is likely to have a pronounced seasonal cycle that should be taken into consideration in both observational and modeling approaches.

Acknowledgments. The author would like to thank Dr. Yves Balkanski for the inspiration, Dr. Hervé Le Treut and Dr. Geneviève Sèze for helpful discussion, and editor James A. Coakley and two anonymous reviewers for their constructive remarks. Computer time for numerical experiments was provided by the Institut du Développement et des Ressources en Informatique Scientifique.

REFERENCES

Albrecht, B. A., 1989: Aerosols, cloud microphysics, and fractional cloudiness. *Science,* **245,** 1227–1230.

Berresheim, H., F. L. Eisele, D. J. Tanner, L. M. McInnes, D. C. Ramsey-Bell, and D. S. Covert, 1993: Atmospheric sulfur chemistry and cloud condensation nuclei (CCN) concentrations over the northeastern Pacific coast. *J. Geophys. Res.,* **98,** 12 701–12 711.

Boucher, O., and U. Lohmann, 1995: The sulfate-CCN-cloud albedo effect: A sensitivity study using two general circulation models. *Tellus,* in press.

Coakley, J. A., R. L. Bernstein, and P. A. Durkee, 1987: Effect of ship-stack effluents on cloud reflectivity. *Science,* **237,** 1020–1022.

Engardt, M., and H. Rodhe, 1993: A comparison between patterns of temperature trends and sulfate aerosol pollution. *Geophys. Res. Lett.,* **20,** 117–120.

Falkowski, P. G., Y. Kim, Z. Kolber, C. Wilson, C. Wirick, and R. Cess, 1992: Natural versus anthropogenic factors affecting low-level cloud albedo over the North Atlantic. *Science,* **256,** 1311–1313.

Fouquart, Y., and B. Bonnel, 1980: Computations of solar heating of the earth's atmosphere: A new parameterization. *Beitr. Phys. Atmos.,* **53,** 35–62.

Han, Q., W. B. Rossow, and A. A. Lacis, 1994: Near-global survey of effective droplet radii in liquid water clouds using ISCCP data. *J. Climate,* **7,** 465–497.

Hartmann, D. L., 1993: Radiative effects of clouds on earth's climate. *Aerosol-Cloud-Climate Interactions,* P. V. Hobbs, Ed., International Geophysical Series, Vol. 54, Academic Press, 151–173.

Hegg, D. A., R. J. Ferek, and P. V. Hobbs, 1993: Light scattering and cloud condensation nucleus activity of sulfate aerosol measured over the northeast Atlantic Ocean. *J. Geophys. Res.,* **98,** 14 887–14 894.

Hunter, D. E., S. E. Schwartz, R. Wagener, and C. M. Benkovitz, 1993: Seasonal, latitudinal and secular variations in the temperature trend: Evidence for influence of anthropogenic sulfate. *Geophys. Res. Lett.,* **20,** 2455–2458.

Jones, A., D. L. Roberts, and A. Slingo, 1994: A climate model study of the indirect radiative forcing by anthropogenic sulphate aerosols. *Nature,* **370,** 450–453.

Kim, Y., and R. D. Cess, 1993: Effect of anthropogenic sulfate aerosols on low-level cloud albedo over oceans. *J. Geophys. Res.,* **98,** 14 883–14 885.

King, M. D., L. F. Radke, and P. V. Hobbs, 1993: Optical properties of marine stratocumulus clouds modified by ships. *J. Geophys. Res.,* **98,** 2729–2739.

Leaitch, W. R., and G. A. Isaac, 1994: On the relationship between sulfate and cloud droplet number concentrations. *J. Climate,* **7,** 206–212.

——, ——, C. M. Banic, and J. W. Strapp, 1992a: Effect of anthropogenic pollution on cloud droplet number concentrations in springtime clouds. *Proc. WMO Workshop on Cloud Microphysics and Applications to Global Change,* Toronto, Ontario, Canada, World Meteor. Org., 25–27.

——, ——, J. W. Strapp, C. M. Banic, and H. A. Wiebe, 1992b: The relationship between cloud droplet number concentrations and anthropogenic pollution: Observations and climatic implications. *J. Geophys. Res.,* **97,** 2463–2474.

Le Treut, H., and Z. X. Li, 1991: Sensitivity of an atmospheric general circulation model to prescribed SST changes: Feedback effects

associated with the simulation of cloud optical properties. *Climate Dyn.*, **5**, 175–187.

Morcrette, J. J., 1989: Description of the radiative scheme in the ECMWF model. ECMWF Tech. Rep. No. 165, 26 pp.

Parungo, F., J. F. Boatman, H. Sievering, S. W. Wilkison, and B. B. Hicks, 1994: Trends in global marine cloudiness and anthropogenic sulfur. *J. Climate*, **7**, 434–440.

Penner, J. E., R. J. Charlson, J. M. Hales, N. S. Laulainen, R. Leifer, T. Novakov, J. Ogren, L. F. Radke, S. E. Schwartz, and L. Travis, 1994: Quantifying and minimizing uncertainty of climate forcing by anthropogenic aerosols. *Bull. Amer. Meteor. Soc.*, **75**, 375–400.

Platnick, S., and S. Twomey, 1994: Determining the susceptibility of cloud albedo to changes in droplet concentration with the Advanced Very High Resolution Radiometer. *J. Appl. Meteor.*, **33**, 334–347.

Quinn, P. K., D. S. Covert, T. S. Bates, V. N. Kapustin, D. C. Ramsey-Bell, and L. M. McInnes, 1993: Dimethylsulfide/cloud condensation nuclei/climate system: Relevant size-resolved measurements of the chemical and physical properties of the atmospheric aerosol particles. *J. Geophys. Res.*, **98**, 10 411–10 427.

Radke, L. F., J. A. Coakley, and M. D. King, 1989: Direct and remote sensing observations of the effects of ships on clouds. *Science*, **246**, 1146–1148.

Sadourny, R., and K. Laval, 1984: January and July performance of the LMD general circulation model. *New Perspectives in Climate Modelling*, A. Berger and C. Nicolis, Eds., Elsevier, 173–198.

Schwartz, S. E., 1988: Are global cloud albedo and climate controlled by marine phytoplankton? *Nature*, **336**, 441–445.

Taylor, J. P., and A. McHaffie, 1994: Measurements of cloud susceptibility. *J. Atmos. Sci.*, **51**, 1298–1306.

Tselioudis, G., A. L. Lacis, D. Rind, and W. B. Rossow, 1993: Potential effects of cloud optical thickness on climate warming. *Nature*, **366**, 670–672.

Twomey, S., 1974: Pollution and the planetary albedo. *Atmos. Env.*, **8**, 1251–1256.

——, 1977: The influence of pollution on the shortwave albedo of clouds. *J. Atmos. Sci.*, **34**, 1149–1152.